

Three-dimensional modulations on the states of polarization of light fields

Peng Li(李鹏), Dongjing Wu(吴东京), Sheng Liu(刘圣), Yi Zhang(章毅), Xuyue Guo(郭旭岳), Shuxia Qi(齐淑霞), Yu Li(李渝), Jianlin Zhao(赵建林)

Citation: Chin. Phys. B . 2018, 27(11): 114201. **doi:** 10.1088/1674-1056/27/11/114201

Journal homepage: http://cpb.iphy.ac.cn; http://iopscience.iop.org/cpb

What follows is a list of articles you may be interested in

Study on polarization properties of graphene coated D-shaped fiber

Xuejing Liu(刘学静), Luwen Yang(杨禄文), Jingyun Ma(马敬云), Caili Li(李彩丽), Wa Jin(金娃), Weihong Bi(毕卫红)

Chin. Phys. B . 2018, 27(10): 104206. **doi:** 10.1088/1674-1056/27/10/104206

Generation of few-cycle radially-polarized infrared pulses in a gas-filled hollow-core fiber

Rui-Rui Zhao(赵睿睿), Zhi-Yuan Huang(黄志远), Ding Wang(王丁), Yu Zhao(赵钰), Yu-Xin Leng(冷雨欣), Ru-Xin Li(李儒新)

Chin. Phys. B . 2018, 27(10): 104204. **doi:** 10.1088/1674-1056/27/10/104204

Linear polarization output performance of Nd: YAG laser at 946 nm considering the energy-transfer upconversion

Jin-Xia Feng(冯晋霞), Yuan-Ji Li(李渊骥), Kuan-Shou Zhang(张宽收)

Chin. Phys. B . 2018, 27(7): 074211. **doi:** 10.1088/1674-1056/27/7/074211

Wideband linear-to-circular polarization conversion realized by a transmissive anisotropic metasurface

Bao-Qin Lin(林宝勤), Jian-Xin Guo(郭建新), Bai-Gang Huang(黄百钢), Lin-Bo Fang(方林波), Peng Chu(储鹏), Xiang-Wen Liu(刘湘雯)

Chin. Phys. B . 2018, 27(5): 054204. **doi:** 10.1088/1674-1056/27/5/054204

Double-rod metasurface for mid-infrared polarization conversion

Yang Pu(蒲洋), Yi Luo(罗意), Lu Liu(刘路), De He(何德), Hongyan Xu(徐洪艳), Hongwei Jing(景洪伟), Yadong Jiang(蒋亚东), Zhijun Liu(刘志军)

Chin. Phys. B . 2018, 27(2): 024202. **doi:** 10.1088/1674-1056/27/2/024202

TOPICAL REVIEW — 80th Anniversary of Northwestern Polytechnical University (NPU)

Three-dimensional modulations on the states of polarization of light fields*

Peng Li(李鹏)[1,†], Dongjing Wu(吴东京)[1], Sheng Liu(刘圣)[1], Yi Zhang(章毅)[1], Xuyue Guo(郭旭岳)[1], Shuxia Qi(齐淑霞)[1], Yu Li(李渝)[1,2], and Jianlin Zhao(赵建林)[1,‡]

[1] *MOE Key Laboratory of Material Physics and Chemistry under Extraordinary Conditions, and Shaanxi Key Laboratory of Optical Information Technology, School of Science, Northwestern Polytechnical University, Xi'an* 710129, *China*

[2] *Department of Public Education, Northwestern Polytechnical University Ming De College, Xi'an* 710129, *China*

(Received 20 July 2018; revised manuscript received 21 August 2018; published online 8 October 2018)

Light fields with spatially structured states of polarization (SoPs) are gathering increasing attention because of their potential applications from optical imaging and micromanipulation to classical and quantum communications. Meanwhile, the concepts within structured light fields have been extended and applied to acoustic, electron, and matter waves. In this article, we review recent developments of the SoP modulation of light fields, especially focusing on three-dimensional (3D) modulations on the SoPs of light fields. The recent progress and novel implementations based on 3D spin-dependent separation are discussed. Following the discussions to this physical phenomenon, we then describe recent developments on the vector fields with 3D structured SoP and intensity distributions, namely, 3D vector fields. The discussed phenomena inspire us to explore other structured light fields for the expansion of applications in biomedical, information science, quantum optics, and so on.

Keywords: polarization, phase, vector field, spin–orbit interaction

PACS: 42.25.Ja, 03.65.Vf, 42.68.Ay, 71.70.Ej **DOI:** 10.1088/1674-1056/27/11/114201

1. Introduction

Polarization, as a basic property of wave, was initially introduced to specify the oscillation orientation of transverse waves. Likewise, for light or other electromagnetic waves, polarization refers to the vibration of the electric field, characterizing the vector property of light waves, and its special role in the light–matter interaction enables many optical devices and systems to be possible. The propagations of polarized light waves and their interactions with various dielectrics have been widely studied, involving the applications in optical measurement, detection, display, and communication, as well as the fundamental realms of material science, astronomy, and biomedicine. In such researches, whether in isotropic or anisotropic materials, the light wave keeps a common feature that its state of polarization (SoP) is homogeneous in the cross-section, such as the linear and circular polarizations.

Some light fields with inhomogeneous SoPs, as special vector solutions of Helmholtz equation, have been extensively studied and demonstrated intriguing phenomena.[1,2] For instance, the radially polarized light field, which has azimuthally variant SoP that depends on the transverse position, remarkably, presents extremely enhanced longitudinal component and sub-diffraction limited focal spot.[3–7] Such fields have been demonstrated with the application prospects in super-resolution imaging and machining, micromanipulation, optical and magnetic recording, and enhanced nonlinear effects.[8–20] Moreover, the spatially structured SoPs within vector fields support another degree of freedom for mode multiplexing and encoding information for optical communication.[21,22] Hence, in the past decade, exploring novel vector fields with remarkable propagating and focusing property was becoming an interesting topic of beam physics.[23–26]

It is well known that light wave is a transverse wave, that is, in free space, its electric vector is perpendicular to the propagation direction. Accordingly, the modulations of SoP mostly devote to engineer light fields with spatially inhomogeneous SoP in the cross-section, including in free space and optical media.[27–44] In other words, the modulations of SoP are limited in two-dimensional plane (i.e., the x–y plane). However, in waveguide and other confined propagating conditions, light fields exhibit nonzero longitudinal components.[45–47] For such special cases, some intriguing physical phenomena, such as transverse spin angular momentum (SAM) and related spin Hall effect of light (SHEL), have been observed.[48–50] On the other hand, under the demands of light manipulation and related applications, the new spatial degree of freedom is increasingly important. Some elaborate vector fields with

*Project supported by the National Natural Science Foundation of China (Grant Nos. 11634010, 11774289, 61675168, and 61377035), the National Key Research and Development Program of China (Grant No. 2017YFA0303800), Joint Fund of the National Natural Science Foundation Committee of China Academy of Engineering Physics (Grant No. U1630125), and the Fundamental Research Funds for the Central Universities, China (Grant No. 3102018zy036).

†Corresponding author. E-mail: pengli@nwpu.edu.cn

‡Corresponding author. E-mail: jlzhao@nwpu.edu.cn

© 2018 Chinese Physical Society and IOP Publishing Ltd

longitudinally variant SoPs have been purposefully proposed, exhibiting new effects and phenomena that can expand the applications and enhance the capability of vector fields.

Moreover, the modulation of SoP in more spatial degree of freedom further reveals the electromagnetic nature of light and enriches the modern optics theory. Remarkably, the fundamental physical theory of spin–orbital coupling has been introduced into steering the SoP.[51–53] In this principle, serials functional elements based on this elegant theory, such as liquid crystal elements,[51,54,55] sub-wavelength gratings,[56,57] and metasurfaces,[58,59] have been proposed, providing effective technical means for many applications, such as spin-dependent holography, information encryption, transmission optical imaging, etc.[2]

In this review, we report on the recent progress in three-dimensional (3D) modulation on SoP of light fields and focus on the evolution dynamics of transverse SoP in 3D space. In Section 2, we discuss the generalized 3D spin-dependent separation, in the consideration of transverse SoP conversion along with beam propagating and focusing. In Section 3, we give an overview of the 3D vector fields, including the vector beams with longitudinally oscillating SoPs and 3D vector focal fields. Finally, we briefly discuss the fundamental and technological challenges, as well as the outlook of anticipated future expansion of the 3D modulation on the SoP.

2. 3D SoP modulations based on spin-dependent separation

Generally, a light beam propagating in free space, as a solution of scalar or vector Helmholtz equation, keeps its SoP upon propagation. However, some light beams with structured SoPs in the cross-section were recently reported to have striking evolution dynamics, e.g., SHEL, that is, two opposite spin components separate from each other with propagating.[60] These typical phenomena are commonly induced by the structured phases arising from the process of polarization conversion. In other words, due to the corresponding relationship between phase gradient in position space and vector in momentum space, various optical elements with specific architectures and phase modulation effects, such as subwavelength gratings,[61,62] metasurfaces,[50] and liquid crystal devices, have been successively reported and demonstrated to be efficient for manipulating the SoP of light fields in 3D.

2.1. PB phase induced spin-dependent separations

The Pancharatnam–Berry (PB) phase, arising from the polarization conversion, has attracted rapidly growing interests in the fundamental physics and SoP modulations.[63–67] Here, we generalize such phenomena and conclude a corresponding modulation model, of which the PB phase generation is schematically illustrated in Fig. 1.[60] As shown, for an incident light field with homogeneous SoP, it can be depicted as $\boldsymbol{E}_{\rm in} = E_0[a\exp(-\varphi_0/2)\boldsymbol{e}_{\rm R} + b\exp(\varphi_0/2)\boldsymbol{e}_{\rm L}]$, where E_0 is the amplitude, φ_0 is a constant phase, a and b are the normalized amplitudes with $a^2+b^2=1$, $\boldsymbol{e}_{\rm R,L}$ denote the right-hand (RH) and left-hand (LH) circular polarizations, respectively.[33,68] Supposing that the two spin states are independently controllable in the polarization conversion process with identical transmission rate and light path, thus the SoP of the output light field is dependent on the phases appending on the two spin components, namely, the PB phases, which are generally described by the solid angles corresponding to the polarization conversion trajectory denoted on the Poincaré sphere, as shown in Fig. 1(b).

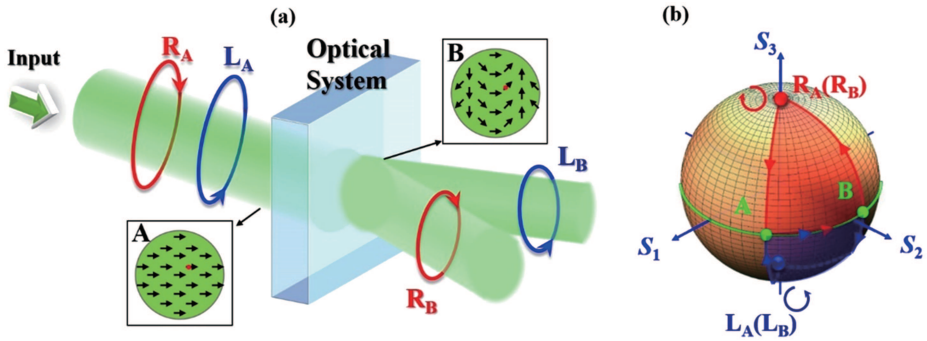


Fig. 1. (color online) (a) Schematic illustration of PB phases arising from polarization conversion and corresponding evolution dynamics of two spin components under the modulation effects of PB phases. (b) PB phases corresponding to the point denoted by red spot in inserts of A and B. R and L denote the RH and LH circular polarizations, respectively.[60]

In general, the polarization conversion shown in Fig. 1(a) can be described by an inhomogeneous half wave plate, which has spatially variant optical axis denoted as $\varphi(x,y)$ but identical transmission rate $t(x,y)=1$. Considering that the LH spin component is input into the system, the corresponding output component can be expressed as[60]

$$\begin{aligned}\boldsymbol{E}_{\rm L} &= \boldsymbol{M}\cdot\boldsymbol{e}_{\rm L} = E_0\begin{bmatrix}\cos 2\varphi & \sin 2\varphi\\ \sin 2\varphi & -\cos 2\varphi\end{bmatrix}\begin{bmatrix}1\\ {\rm i}\end{bmatrix}\\ &= E_0\exp({\rm i}2\varphi)\boldsymbol{e}_{\rm R},\end{aligned} \tag{1}$$

where $\boldsymbol{M}$ is the Jones matrix of the inhomogeneous wave

plate. Equation (1) clearly indicates that the LH spin component obtains an additional phase denoted as $\psi_L = 2\varphi(x,y)$, this special phase arising from polarization conversion is the very PB phase. Moreover, it is notable that this component flips the SoP into a RH circular one. Likewise, the RH spin component obtains an additional phase denoted as $\psi_R = -2\varphi(x,y)$ and transforms into a LH circular polarization. Supposing $a = b = 1/\sqrt{2}$, the output field immediately from the optical system can then be consequently described as

$$\begin{aligned} \boldsymbol{E}_{\text{out}}(x,y) &= E_0\left[e^{i(\psi_L-\varphi_0)}\boldsymbol{e}_L + e^{i(\psi_R+\varphi_0)}\boldsymbol{e}_R\right]/\sqrt{2} \\ &= E_0 e^{i\left(\frac{\psi_R+\psi_L}{2}\right)}\left[\cos\left(\frac{\psi_R-\psi_L}{2}+\varphi_0\right)\boldsymbol{e}_x \right. \\ &\quad \left. + \sin\left(\frac{\psi_R-\psi_L}{2}+\varphi_0\right)\boldsymbol{e}_y\right]. \end{aligned} \tag{2}$$

Equation (2) indicates that the output field transfers local SoP along an angle $(\psi_R - \psi_L)/2 + \varphi_0$, but keeps its intensity profile at the immediate output plane. Importantly, the appending phases ψ_R and ψ_L, i.e., the PB phases, make it possible to control the evolution of the two spin components by engineering phase structures, resulting in intriguing phenomena such as spin-dependent separation and spin-dependent guiding.[69–72] Take the typical selection of PB phase that has a linear function as an example, e.g., $\psi_{L,R} = \pm k_x x$. For this case, two spin states would obtain two mutually conjugate titled phases, resulting in the transverse separation with each other upon propagation. Such a macroscopic spin-dependent dynamic of light was firstly implemented by Hasman using spatially variant subwavelength grating.[73] Remarkably, Zhang *et al.* observed extremely enhanced spin-dependent transverse separation by using meatsurface based on PB phase theory.[74] Ling *et al.* reported a giant spin-dependent separation by using dielectric metasurface fabricated by the femtosecond laser self-assembly nanostructure.[75] Analogous to the dynamic behavior of spin electrons in solid-state system, i.e., spin Hall effect, such kind of transverse separation, referring to two opposite spin states of light, is also named as SHEL.[76–78]

In addition, combining the linear phase with spiral phase, we realized the manipulation of SAM and OAM separation simultaneously. For instance, figure 2 displays the transverse separation of two constituent components with opposite SAMs and OAMs.[60] Figure 2(a) depicts the intensity and polarization distributions at the output plane of polarization conversion system. For such a special case, the PB phases are designed as $\psi_{L,R} = \pm(k_x x + \phi)$. As a result, the resultant field presents a hollow core, and horizontally variant SoP. Figures 2(b)–2(d) display the experimentally measured two constituent components, SoP distributions, and evolution process, respectively. Clearly, two components carrying opposite OAMs occur spin-dependent separation upon propagation, under the modulation of linear PB phase.

Owing to the geometric flexibility, the PB phase was further designed to realize fetching modulation, e.g., longitudinal spin-dependent separation.[60] Two conjugate spherical phases that enable the shift of focal length are introduced into PB phases, for which the convergence and divergence phases denoting as $\psi_{L,R} = \pm(\alpha r^2)$ are encoded into a square phase of $\exp(i\alpha r^2)$. For this case, two spin components respectively focus into the focal planes $f(\alpha_0 \pm \alpha)$, resulting in the longitudinal spin-dependent splitting. According to this principle, Hasman *et al.* created PB phase lens element composed by subwavelength grating with radially variant orientation.[79,80] When illuminating this PB phase element, longitudinal multi focal spots with variant SoP appear. Furthermore, the PB phase-based multi-foci lens has also been realized by using segmented metasurface with azimuthally variant phase modulation effect.[81] Interestingly, such multi-focal polarization-dependent lens generates focal field with longitudinally variant spot number and SoP that depend on the degree of polarization of incident beam.

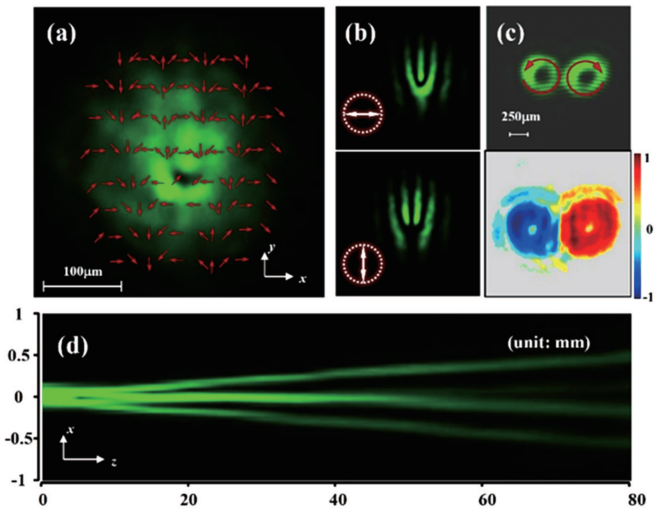


Fig. 2. (color online) Spin-dependent separation induced by PB phases upon propagation. (a) Initial field with polarization direction marked by red arrowheads. (b) Horizontally and vertically polarized components of output beam. (c) The distribution of output beam after propagation (top), and the corresponding S_3 distribution (bottom). (d) Side view of the beam propagation.[60]

Beyond that, combining this longitudinal spin separation with the transverse one, it is possible to achieve arbitrary spin-dependent separation in 3D space.[60] The PB phase in this case can be expressed as a polynomial like $\psi_R = k_x x + k_y y + \alpha r^2$. The first two terms and the third term are the phase factors of plane and spherical waves, respectively, providing three degrees of freedom along x, y, z axes to control the spin-dependent separation in 3D space. The positions of focal points (x_R, y_R, z_R) and (x_L, y_L, z_L) are determined by the parameters k_x, k_y, α, following $x_{R,L} = k_x z_{R,L}/k$, $y_{R,L} = k_y z_{R,L}/k$,

and $z_{R,L} = f(\alpha_0 \pm \alpha)$. Figure 3 shows an experimentally measured 3D spin-dependent separation. Obviously, this spin-dependent separation increasing along z direction actually performs an equivalently longitudinal SoP modulation. As above presentation, this modulation principle has been successively applied to various functional elements for the implementations such as geometric-phase lens and prism, spin-dependent hologram, and so on.

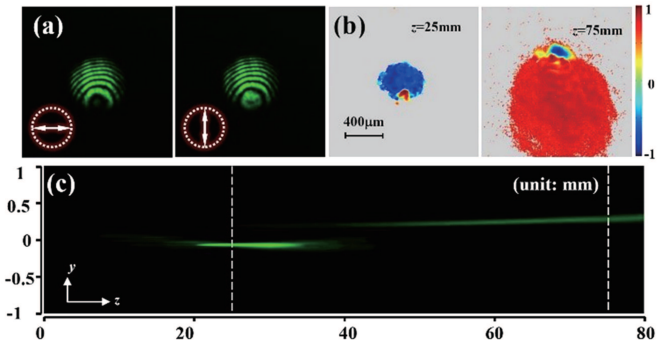


Fig. 3. (color online) 3D spin-dependent separation. (a) Horizontally and vertically polarized components. (b) Distributions of S_3 at $z = 25$ mm and 75 mm. (c) Side view of intensity evolution in the x–z plane.[60]

2.2. Wave front modulation induced spin-dependent separations

In addition to the PB phase modulation strategy, some modulations affecting the wave front of vector beams have also been reported to achieve spin-dependent separation. Similarly, these methods are both based on the principle that the vector beam is the coaxial superposition of two spin components carrying opposite spiral phases. For a cylindrical vector beam, two opposite spin components generally have equivalent phase topological charges, i.e., $|l_R| = |l_L|$, exhibiting identical propagation dynamics.[68,82–84] As a whole, the SoP in the cross-section remains invariant during propagation. However, once the vector beam has an additional phase, e.g., the vector vortex beam, of which two spin components have different topological charges, i.e., $|l_R| \neq |l_L|$, these distinct phases will significantly influence the evolutions of the two spin components due to the strong dependence of cross-sectional intensity profile and Gouy phase on the topological charge.[82,85–87] That is, the two spin components that compose the vector vortex beam do not keep identical intensity profiles and dynamic phases during propagation. Meanwhile, considering the rotational symmetry, the two spin components consequently occur radial spin-dependent separation. As a whole, the vector vortex beam simultaneously presents radially and longitudinally variant SoP.

We note that, such a z-dependent variation has the maximum effect at far-field, i.e., $z \to \infty$. In experiment, the Fourier transform with a lens is a common method to achieve such a special condition. We demonstrated such kind of spin-dependent separation and 3D SoP variation by detecting the SoP distribution at the Fourier plane of vector vortex beams.[88] Figure 4 shows the experimentally measured SoP transition of focused vector vortex beams with different polarization orders and phase topological charges. The corresponding theory and experiment results show that, the SoP transition is related to the parity of smaller modulus between polarization order m and topological charge l. Moreover, the focal fields of vector vortex beams show radially variant polarization distributions resulting from the unequal intensity proportion of two spin components, namely, radial spin-dependent separation. Remarkably, this radial spin-dependent separation has been successfully used to enrich the optical manipulation of micro-particles[89] and construct focal fields with typically spatial properties.[90,91]

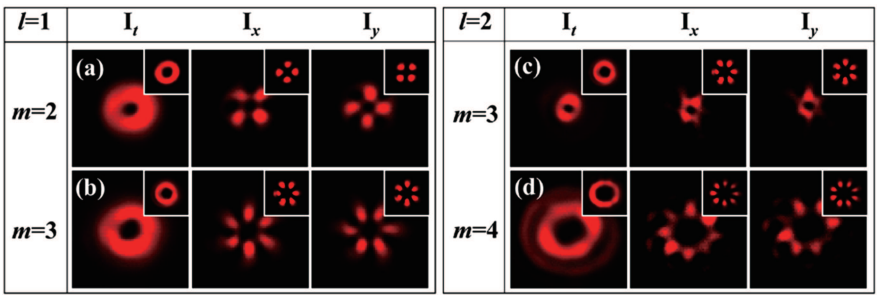


Fig. 4. (color online) SoP transition of vector vortex beams with different polarization orders and topological charges. The polarization order and topological charge are denoted as m and l, respectively.[88]

The caustic phases,[92] which produce significant evolution dynamics such as arbitrary curve trajectory and transverse acceleration,[93–100] have recently been introduced into vector beams to manipulate SoP, SAM and OAM fluxes in 3D space, producing physical interests such as spin–orbit interaction and polarization singularities conversion. Figure 5 shows the autofocusing of radially polarized Airy beams without and with a single charged spiral phase.[101] From the experimental results, it is clear that, under the modulation of spiral phase, the radially polarized autofocusing Airy beam occurs abrupt polarization transition, associated with spin–orbit interaction. Likewise, this impressive phenomenon has been revealed ac-

cording to mode superposition theory. However, it is noteworthy that, when the attached topological charge and the polarization order of the Airy beam are equal in number, the local SoP undergoes an abrupt transition from linear to circular polarization at the focal point, exhibiting an intuitional result that the associated OAM partially coverts into the spin of photons.

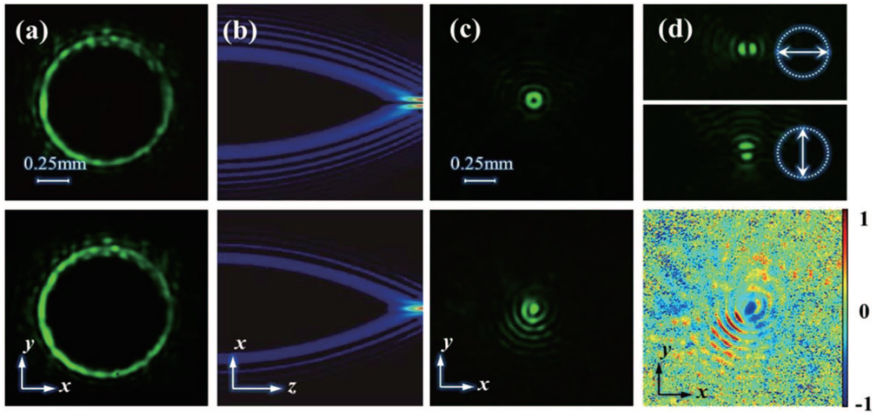


Fig. 5. (color online) Autofocusing of radially polarized Airy beams without (top) and with (bottom) a single charged vortex phase. (a) and (c) Intensity patterns at pupil and focal planes, respectively. (b) Side view of the beam propagation from numerical simulation. (d) Measured beam polarizations at focal plane.[101]

We have further encoded complex caustic phases onto the vector vortex beams. Figure 6 shows the spin-dependent separation of vector abruptly autofocusing beam encoding with cosine-azimuthal variant phase denoted as $\Phi = \cos(n\varphi)$.[102] Obviously, the spin-dependent separation induced by this typical caustic phase presents strong dependence on the parity of factor n. This relationship was approximately mapped by employing the local spatial frequency, which establishes a simple mapping relationship between the focal field intensity and the pertinent phase distribution of the input field.[99] According to this theoretical principle, focal fields with desirable intensity, SoP, and phase structures were realized by consciously managing the cosine-azimuthal phase. Actually, this mapping theory supplies a commonly inverse approach to engineer the caustic phase, for the steering of spin–orbit interaction and optical micro manipulation.[103,104]

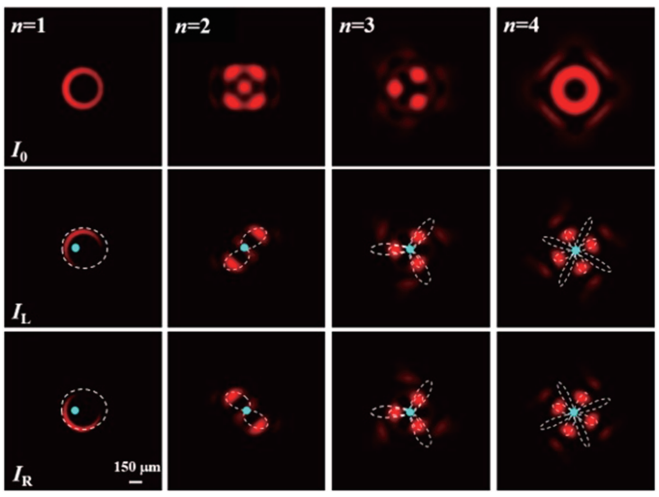


Fig. 6. (color online) Cosine-azimuthal phase modulated spin-dependent separation of vector autofocusing Airy beams with polarization order of $m = 2$. The top, middle, and below rows correspond to the intensity patterns of total, RH, and LH circularly polarized components, respectively.[102]

Moreover, it is possible to steer the spin-dependent separation by modulating the amplitude profile of vector beams in the cross-section. Owing to the rotational symmetry of cylindrical vector beams, various amplitude modulations aiming to break this property have been proposed, resulting in conceptual and application interests.[82–84,105,106] Remarkably, the fan-shaped masks that have sectorial photic region, attaching onto a vortex beam, produce transverse energy flow to gradually transfer the energy to the opaque region upon beam propagation.[105] Figure 7 schematically illustrates the transverse energy flow induced spin-dependent separation of cylindrical vector beam, under the amplitude modulation of a fan-shaped mask.[106] As shown, two spin components carrying opposite spiral phases take opposite angular rotations, under the effect of transverse energy flow arising from the symmetry broken of OAM.

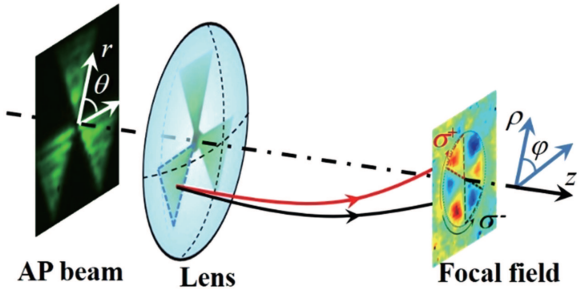


Fig. 7. (color online) Schematic illustration of spin-dependent separation of azimuthally polarized (AP) beam induced by amplitude modulation.[106]

This diffraction dynamic can be semi-quantitatively described by the angular diffraction theory.[105] That is, after the fan-shaped aperture, the transmitted field can be described as a series of OAM spectra, with distinct complex amplitudes and topological charges. Then the total diffraction field is the superposition of these diffractive OAM spectra, which can

be described by the Fresnel diffraction theory. According to this, we proposed a theoretical model for explicitly explaining the diffractive dynamics of azimuthally broken vector vortex beams.[105] This model reveals that the spin-dependent azimuthal separation is closely related to the polarization order of the modulated vector beam and the diffraction distance. The results shown in Fig. 8 are the dependence of rotation angle of two spin components on the polarization order and diffractive distance.[82] For the vector beams carrying zero OAM, two spin components rotate equivalent angles along opposite azimuthal directions. While for the vector vortex beams carrying nonzero OAM, the additional OAM enables the manipulation of spin-dependent separation, namely, the angle width between two spin components.[107]

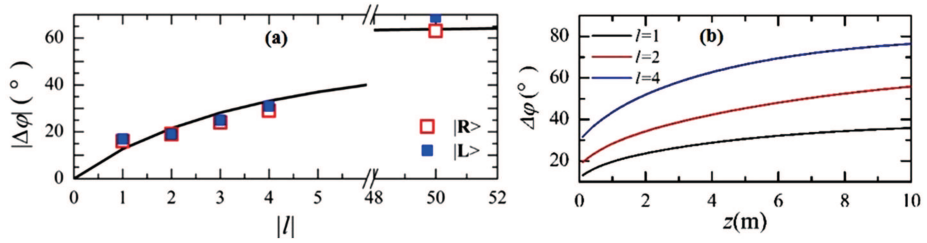


Fig. 8. (color online) Rotation angle $|\Delta\varphi|$ versus the (a) polarization order $|l|$ and (b) diffractive distance of fan-shaped vector beams. The diffractive distance corresponding to (a) is $z = 25$ cm, and the angular widths of photic regions are $\pi/2$.[82]

From the results shown in Fig. 8(b), it can be concluded that the rotation angle has the maximum value of $\pi/2$ at far-field. This means that the spin-dependent azimuthal separation reaches its maximum value of π. This phenomenon has been demonstrated in the focal field of azimuthally broken vector vortex beams. According to this principle, some rotationally symmetric amplitude and phase masks, as well as vector beams with multiple singularities, have been proposed to redistribute SAM, OAM, and energy flow in the focal plane.[41,108–110] Interestingly, this modulation method and controllable spin-dependent separation have been demonstrated with the application possibility in optical information process.[111]

3. 3D vector beams

The above discussed 3D varying SoP mainly arises from the off-axial superposition of two spin components, that is, the accumulated spin-dependent displacement. Besides this, various vector beams consisting of two coaxially superposed spin components, with longitudinally variant SoP, have been proposed.[104,112–118] These vector beams with 3D designed SoP and intensity structures are also named as 3D vector beams, exhibiting quite attractive potentials for a variety of practical applications such as optical trapping, atom lithography, quantum information processing, optical machining, and light–matter interaction.

3.1. 3D vector beams based on longitudinal amplitude modulations

To construct a vector beam with longitudinally variant SoP, we started from the SoP description method.[119] Figure 9 depicts the common Poincaré sphere description method of SoP. Each point on the Poincaré sphere, denoting by angular position $(2\varphi, 2\chi)$, corresponds to one SoP that consists of arbitrary two bases with orthogonal SoPs, that is, two points that are centrally symmetric with respective to the sphere center.[120] For instance, two crossing points of prime meridian and equator that correspond to the horizontally and vertically polarized states are a pair of bases. Accordingly, each point on the spherical shell can be decomposed into these two bases with variant amplitude ratio or phase difference.

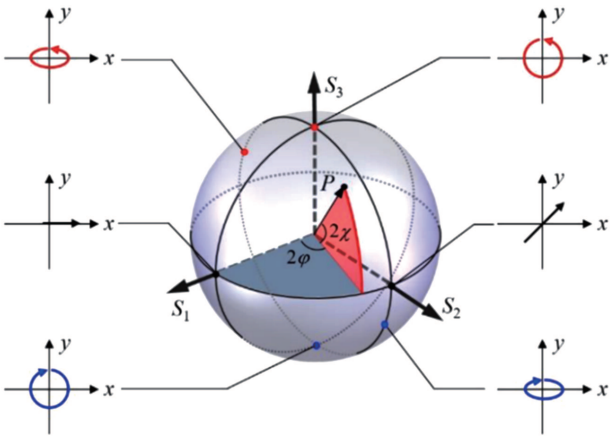


Fig. 9. (color online) Poincaré sphere description method of SoP.

For simplicity, we coaxially superposed two constituent beams with opposite linear polarizations, i.e., the horizontally and vertically linear polarizations, and supposed these two constituent beams having Bessel functional intensity profiles in the cross-section. It is well known that, Bessel beams are spatially structured beams with the property of non-diffraction and self-healing, typically maintaining their SoP during propagation.[121–128] Based on this, we further assumed that the total field has a Bessel profile and longitudinally varying SoP, the electric field $\boldsymbol{E}$ can thus be expressed as[112]

$$\boldsymbol{E}(r,z) = \exp\left(-\frac{r^2}{w_0^2}\right) J_0(k_r r)\exp(\mathrm{i}k_z z)$$

$$\times \begin{bmatrix} E_{\mathrm{H}}(z)\,\mathrm{e}^{\mathrm{i}\delta_{\mathrm{H}}(z)} \\ E_{\mathrm{V}}(z)\,\mathrm{e}^{\mathrm{i}\delta_{\mathrm{V}}(z)} \end{bmatrix}, \tag{3}$$

where $E_{\mathrm{H,V}}(z)$ are normalized on-axis field distributions (axial envelopes) corresponding to the horizontally and vertically polarized bases, respectively, and $\delta_{\mathrm{H,V}}(z)$ are phase retardations independent of dynamic phases. The SoP depending on the Jones vector can be intuitively characterized by the ellipse angle χ and orientation angle ψ, which are given by

$$\begin{aligned} \sin 2\chi &= \frac{2E_{\mathrm{H}}E_{\mathrm{V}}\sin(\delta_{\mathrm{H}}-\delta_{\mathrm{V}})}{E_{\mathrm{H}}^2+E_{\mathrm{V}}^2}, \\ \tan 2\psi &= \frac{2E_{\mathrm{H}}E_{\mathrm{V}}\cos(\delta_{\mathrm{H}}-\delta_{\mathrm{V}})}{E_{\mathrm{H}}^2-E_{\mathrm{V}}^2}. \end{aligned} \tag{4}$$

Equation (4) clearly provides two schemes to steer the longitudinal variation of SoP, that is, engineering two components with z-dependent axial envelopes and phase difference, i.e, ensure $E_{\mathrm{H}}(z)/E_{\mathrm{V}}(z) \neq$ const. or $\delta_{\mathrm{H}}(z)-\delta_{\mathrm{V}}(z) \neq$ const.

As is well known, any azimuthally independent field can be divided into a serial of Bessel spectra. This means that the constituent Bessel beams described in Eq. (3), with varying axial envelops denoting as $E_{\mathrm{H,V}}(z)$, can be constructed from the superposition of Bessel functional spatial spectra.[129] Accordingly, the spatial spectra can be created based on the inverse Fourier transform expressed as[112]

$$\begin{aligned} &U_{\mathrm{H,V}}\left(\sqrt{k^2-k_z^2}, z=0\right) \\ &= \frac{1}{2\pi k_z}\mathcal{F}^{-1}\left[E_{\mathrm{H,V}}(z)\exp(\mathrm{i}k_{z0}z)\right]. \end{aligned} \tag{5}$$

The corresponding modulation mechanism is schematically illustrated in Fig. 10. As shown, a linearly polarized input beam is split into horizontally and vertically polarized beams, then two constituent beams after independently spatial spectrum modulation are transformed into two quasi-Bessel beams with pre-shaped axial envelops.[112] Note that, here we engineered two constituent beams having complementary intensity profiles, which enables the total field to present longitudinally variant SoP and uniform intensity profile. Clearly, the axial variation of intensity ratio results in the longitudinal variation of SoP. With this method, we constructed zeroth order quasi-Bessel beams with uniform axial intensity but longitudinally varying SoP. Moreover, we demonstrated the possibility and flexibility of manipulating the trajectory, speed, and period of SoP transformation by changing the basis states, axial envelopes, and initial phases.

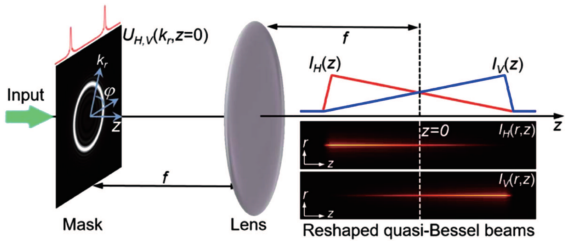


Fig. 10. (color online) Schematic illustration of reshaping the axial intensity envelops of quasi-Bessel beams.[112]

There is another implementation method for functional intensity envelope, the Frozen wave (FW),[130–132] which consists of a suitable superposition of co-propagating Bessel beams with equal frequency but different transverse and longitudinal wavenumbers, having the advantages of static envelope and arbitrary adjustable longitudinal intensity pattern. Furthermore, the FWs have been successively designed to construct 3D vector beam with higher polarization order. The electric field of FW composed by $2N+1$ Bessel beams of order l can be given as[131]

$$F_l(\rho,\phi,z,t) = \mathrm{e}^{-\mathrm{i}\omega t}\sum_{j=-N}^{N} A_j J_l(k_{lj}\rho)\,\mathrm{e}^{\mathrm{i}k_{zj}z}\,\mathrm{e}^{\mathrm{i}l\phi}, \tag{6}$$

where A_j is the weighting factor for Bessel spectrum, determined by the distribution of desired light field. Figure 11 schematically shows the construction principle based on the FWs with sinusoidal functional axial envelopes and opposite spin states.[117] Suppose that two FWs have a constant phase difference $\varphi_0 = -\pi/2$ and independent OAMs denoting as $m\hbar$ and $n\hbar$. Therefore, the composed field varies its inhomogeneous SoP along the red trajectory on the hybrid order Poincaré sphere,[133–135] as shown in Fig. 11(b).

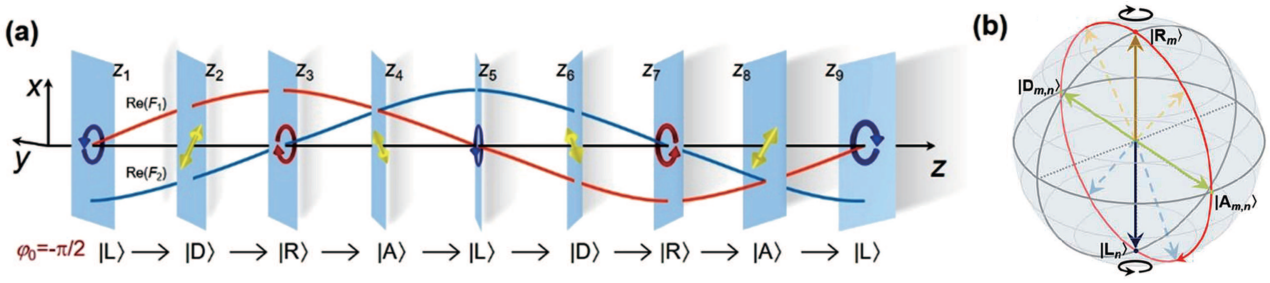


Fig. 11. (color online) (a) Schematic diagram of polarization oscillating vector beam based on Frozen waves. (b) SoP oscillating trajectory on the hybrid order Poincaré sphere.[117]

Combining above schemes, a new class of 3D vector beams with longitudinally oscillating SoP within centimeters spatial interval have been proposed via the superposition of two co-propagating optical FWs with pre-shaped axial envelopes and transverse phase structures. The results shown in Fig. 12 are the experimentally measured SoP and Stokes parameter S_3 distributions at four transverse planes with equivalent interval. The initial conditions are $\varphi_0 = -\pi/2$ and $m = -n = 1$. In such a special case, the oscillation trajectory corresponds to the red curves shown in Fig. 11(b), but on a first order Poincaré sphere, on which the diagonal and antidiagonal points denote the first order hybrid states, as shown in Figs. 12(a) and 12(b), respectively. Considering the static property of FWs, we defined these two states as nodes, while the pole states corresponding to homogeneous circular polarization as antinodes. As the experimental results shown, the composed field longitudinally oscillates its transverse SoP between nodes and antinodes. Consequently, we defined such 3D vector beams as polarization oscillating beams.

Furthermore, we created other kinds of polarization oscillating beams with fundamental and higher order SoPs to demonstrate the feasibility of our approach. Likewise, Corato–Zanarella *et al.* reported similar 3D vector beams constructed from FWs with another pre-shaped axial envelops. It is obvious that this method has the ability to construct 3D vector beams with uniform and other functional axial intensity, which are particularly useful for many applications such as optical manipulation, light guiding of atoms, polarization-sensitive sensing, and so on.[118]

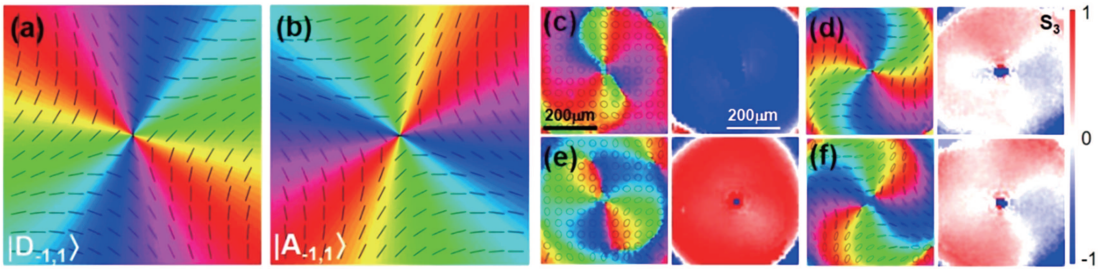


Fig. 12. (color online) Experimentally measured SoP distributions at two adjacent (a) nodes and (b) antinodes. (c)–(f) Left, polarization orientation (background) and polarization ellipticity distributions; right, S_3 distributions. Black line and ellipse depict the linear and ellipse polarizations, respectively.[117]

3.2. 3D vector beams based on longitudinal phase modulations

Besides the amplitude modulation, some attention has been devoted to the modulation of phase along propagation direction. Several modulation mechanisms have been proposed to construct 3D vector beams. Remarkably, Moreno *et al.* proposed 3D vector beams by engineering axicon phase profiles for two orthogonally polarized constituent beams.[113,114] The construction principle is schematically shown in Fig. 13. The modulation phases attached onto two constituent beams are $\Phi_{1,2}(r,\phi,z=0) = \pm(l\phi + \pi r/d)$, with a radial period of d. Meanwhile, such two constituent beams are linearly focused into lth order Bessel beams with longitudinally varying phases $\Phi_{1,2}(r,\phi,z) = \pm(l\phi + \pi z/\Lambda)$, after an axicon or equivalent concial phase, as shown in Fig. 13(a).[115] For such a specific case, considering the local SoP at one point in the cross-section, it periodically varies along the propagation direction, as schematically shown in Fig. 13(b). As a whole, the vector beam presents 3D variant SoP. Employing this transverse-to-longitudinal structuring strategy, we created zeroth and higher order vector Bessel beams with 3D variant SoP. Figures 13(c)–13(h) display the experimental results of a zeroth order vector Bessel beam.

Furthermore, we explored the self-healing of these vector Bessel beams. Figure 14 depicts the measured reconstruction of zeroth order vector Bessel beams after a circle obstacle.[115] The results show that, similar to the self-healing of their intensity profiles, the spatial property of SoP, especially the SoP z-dependence can self-heal. This self-healing capability is important in practical applications of light–matter interaction at micro scalar.

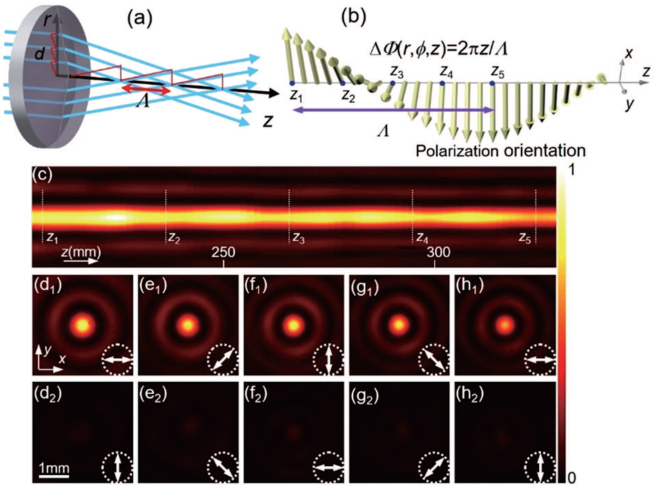


Fig. 13. (color online) (a) Construction principle of 3D vector beams based on longitudinally variant phases. (b) Local polarization orientation in the cross-section versus propagating distance. (c) Intensity profile in the y–z plane of zeroth order vector Bessel beam. (d)–(h) Intensity distributions in the cross-section after a polarizer at different propagation distances shown in (c). The arrows in (c)–(h) denote the polarization orientation of the polarizer.[115]

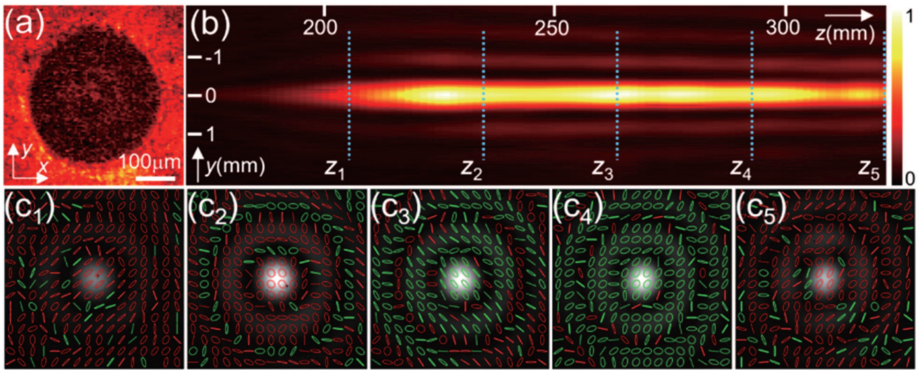


Fig. 14. (color online) Measured reconstruction of zeroth order vector Bessel beams after a circle obstacle. (a) Intensity distribution immediately after the obstacle. (b) Intensity distribution in the y–z plane after the obstacle. (c_1)–(c_5) The reconstructed beams at planes z_1 to z_5 denoted in (b), respectively.[115]

It is noteworthy that, the above described 3D vector beams composed by co-propagating constituent beams with pre-shaped axial envelops or phase structures have controllable periods, e.g., the polarization oscillating beams. However, two counter-propagating circularly polarized beams with different amplitude ratios and phase structures have also been proposed to construct 3D vector beams, e.g., vector standing waves with periodically oscillating SoPs.[136] This special field is also named as superspiral light,[137] because its oscillating period of SoP is shorter than the wave length. This continuous change of SoP along the axial direction produces polarization gradient,[138] exhibiting application potential in optical lattices for sub-Doppler cooling of atoms.[139,140] Remarkably, cylindrically symmetric 'Sisyphus' and 'corkscrew' types polarization gradients have been constructed based on the superposition of counter-propagating vector Laguerre–Gauss (LG) beams with different types of SoPs,[141–143] such as the radially and azimuthally polarized LG beams.

Most recently, the 3D vector beams, configured from the counter-propagating cylindrical vector beams, have been proved the entanglement dynamics in free space under unitary conditions.[144] Due to the non-separability of cylindrical vector vortex fields,[145,146] the longitudinally oscillating SoP structure produces oscillating degree of local entanglement during propagation in free space, as a result of spin–orbit interaction. Figure 15 shows the schematic representation of the 3D vector field with a z-dependent degree of entanglement. Such a 3D vector field is equivalently composed by two counter-propagating fields with radially and azimuthally polarized SoPs. As shown in top three rows, the z-dependent dynamic phases produce the longitudinal variation of transverse SoP structures, that is, the SoP oscillates between fully vector and fully scalar modes. Notably, during propagation, the total angular momentum is constant, i.e., $J_z = 0$, indicating the periodic coupling between SAM and OAM. As a result, the degree of entanglement oscillates periodically along the propagation direction. This classical entanglement dynamic arising from the 3D SoP property gives a new insight of spin–orbit coupling of light and offers a new tool to enrich the application of structured fields.

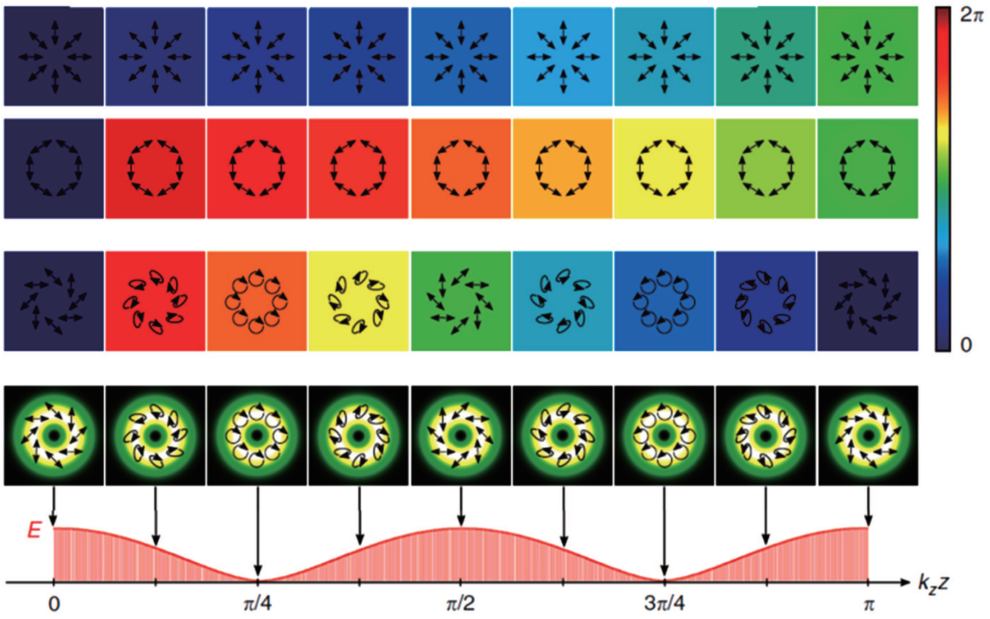


Fig. 15. (color online) Schematic representation of a 3D vector field with z-dependent degree of entanglement.[144]

Different from the additional phase strategy, the Gouy phase,[147] a typical part of dynamic phase that nonlinearly increases with beam propagating, has also been reported to construct 3D vector beams,[148–150] because of its close dependence on the mode orders,[151] i.e., the radial and azimuthal orders denoted as p and l, respectively. For instance, Cardano *et al.* generated Poincaré beams that rotate transverse SoP distribution with beam propagating by coaxially overlapping the $LG_{0,0}$ and $LG_{0,l}$ modes. Utilizing a spiral wave plate, the incident light field with $LG_{0,0}$ mode is partly transformed into the $LG_{0,l}$ mode carrying a vortex phase. Then it axially overlaps with the idle part of $LG_{0,0}$ mode, resulting in Poincaré beam with lemon, star, and spiral polarizations that depend on the topological charge of the $LG_{0,l}$ mode. In this process, an extra phase difference emerges with the expression of $\Delta\Phi = |l|\tan^{-1}(z/z_0)$, called Gouy phase shift. This z-dependent phase difference gives rise to the rotation of polarization upon beam propagation. Figure 16 shows the variations of transverse SoP of Poincaré beams with lemon, star, and spiral SoP structures.[149]

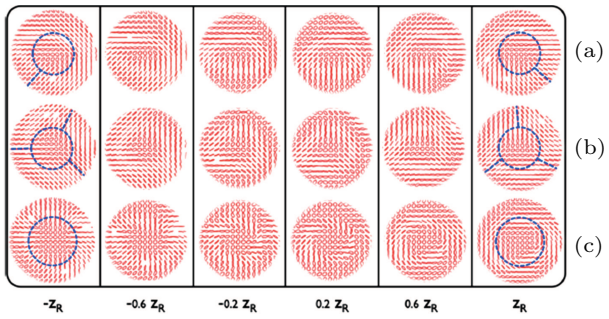


Fig. 16. (color online) Variations of transverse SoP of Poincaré beams with (a) lemon, (b) star, and (c) spiral SoP structures, respectively.[149]

3.3. 3D vector focal fields

Since the cylindrically polarized beams present intriguing tightly focusing property, the research referring to tightly focusing of light fields is one of the most attractive topics in optics. As is well known, the tightly focused field of radially polarized beam presents a much smaller focal spot, supplying a desirable protocol for super-resolution imaging and lithography. Importantly, such a focal field has an extensively enhanced longitudinal component, for which conceptual interests such as transverse SAM[152–154] and Möbius trip[155] have been reported. According to such two typical features of tightly focused vector beams, considerable tightly focused fields with specific intensity, polarization, phase structure, as well as energy flow distribution, by means of amplitude and phase modulations in the pupil plane,[13,156–159] have been proposed toward promising applications such as super-resolution imaging, optical trapping, and machining.

Obviously, constructing focal field with 3D SoP structure, even geometrical angular momentum in the space near focal plane, would supply more vector beams and further enrich the light–matter interaction.[160–162] For instance, the enhanced longitudinal component has application interests in light–matter interaction, which benefits polarization information encryption with ultra-security and optical manipulation of micro-particles (Fig. 17).[162]

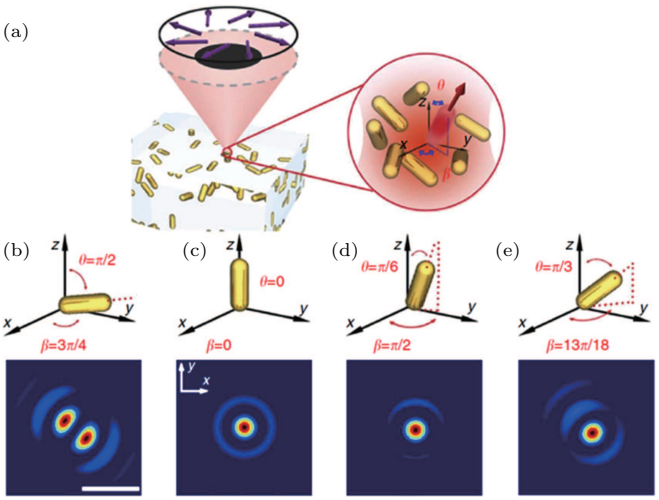


Fig. 17. (color online) 3D alignment determination of single gold nanorods in two-photon fluorescence scanning images. (a) Schematic illustration of an arbitrary 3D polarization beam interacting with randomly aligned gold nanorods. (b)–(e) Schematic 3D alignment of gold nanorods and their associated calculated fluorescence rate images.[162]

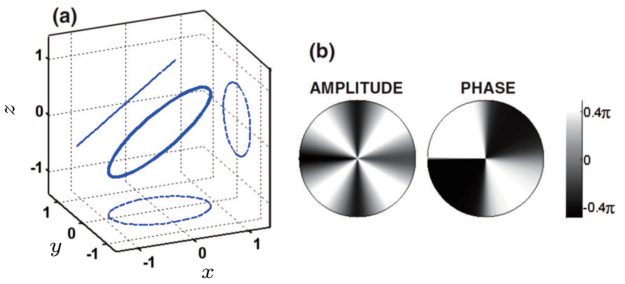


Fig. 18. (color online) (a) An example of 3D SoP and its projections on three orthogonal planes. (b) The corresponding amplitude and phase distributions of incident field.[163]

Controlling the focal field with arbitrary 3D SoP in the vicinity of focus has attracted extensive researches recently. For instance, Abouraddy *et al.* proposed an approach to optical microscopy that enables full control over the 3D SoP at the focal spot by controlling the azimuthal harmonic content of the input field.[163] Figure 18 shows the resultant 3D vector focal field. As shown, the projected SoP is elliptical in the x–y plane, circular in the y–z plane, and linear in the x–z plane. By combining the electric dipole radiation and a vector diffraction method, Chen *et al.* proposed an analytical approach for full control over the 3D SoP and field distributions near the tight focus.[164] Moreover, Zhu *et al.* reported focal fields with tunable 3D SoPs in 4Pi focusing system by uniformly modulating the amplitude or polarization of one half of

the input beam.[165] Utilizing this focusing scheme, tightly focused fields with special 3D SoP and SAM distributions have been proposed.

The promising applications of 3D vector focal fields motive researchers to find a generalized engineering scheme.[166] Subsequently, inverse design methods, namely, reverse engineering approaches, for complete shaping of the focal field with prescribed distribution of intensity, phase, and SoP, have been proposed.[167,168] Most recently, Ding *et al.* further presented a method of shaping 3D vector focal field with controllable SoP variation along arbitrary curves in 3Ds.[169] Two curved laser beams with orthogonal polarizations and predesigned intensity and phase structures were coaxially superposed to produce a 3D vector focal field. Figure 19 gives the experimental results of the generated vector Archimedean spiral (left) and the hybrid vector beams (right), of which the linear polarization state varies continuously along the curve. This efficient and noniterative method exhibits application potentials in realms related to optical data storage, microscopy, material processing, and optical tweezer.

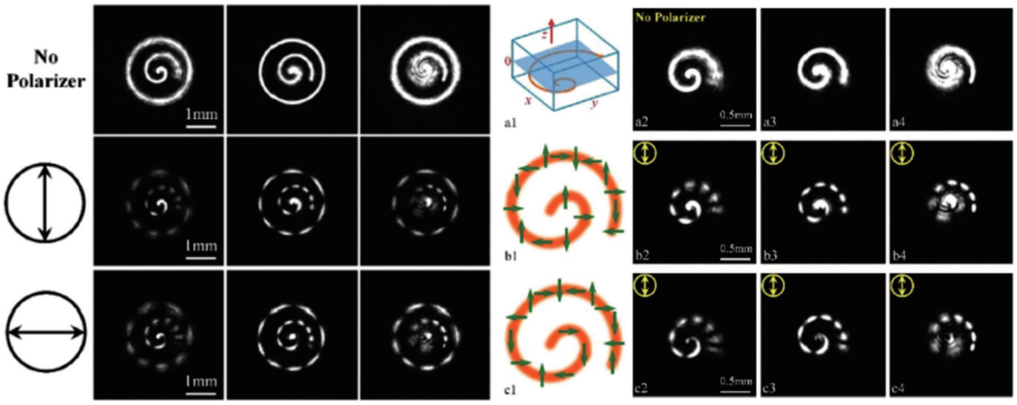


Fig. 19. (color online) Experiment results of the generated vector Archimedean spiral, where the linear polarization state varies continuously along the curve.[169]

4. Conclusions

Since the first demonstration of radially polarized laser mode in 1972,[170] a great variety of efforts have been devoted to exploiting the polarization modulation of light field, as well as the propagation characteristics and focusing properties of polarization structured light field. Various structured light fields with novel diffraction and mechanical properties, as well as momentum and angular momentum distributions, have been proposed and demonstrated in the application realms in optical manipulation, optical imaging, optical information communication, optical detection, optical processing, etc. Going forward, the modulation referring to more degree of freedom is becoming one of the prospects of structured light fields. Especially, the modulation on the longitudinal direction, producing novel structured fields such as super-spiral field, will afford further opportunities for the light–matter interaction, e.g., enhanced circular dichroism and longitudinal super-resolution in light-sheet microscopy. Therefore, the longitudinal modulation on the polarization is still in its infancy.

Spin–orbit interaction in more degree of freedom associated with SoP conversion may potentially allow the discovery of new physics, with opportunities for highly sensitive measurements, and enhanced light–matter interaction in linear and nonlinear optics. Meanwhile, with the rapidly developed technology in nanofabrication, exploring integrated and efficient optical elements for multiple parameters modulation in 3D is considerably attractive. Additionally, the combined modulation referring to time domain parameters of light field will create beams with impressive optical features.[171] The related 3D modulation mechanisms of light field will open the route toward new findings in other waves, such as acoustic waves, water waves, electron waves, and matter waves.

Acknowledgment

The authors would like to thank Lei Han, Huachao Cheng, Gaofeng Xie, Peng Li, Wei Zhang, and Xiangyang Jiao for the earlier contributions in the laboratory.

References

[1] Zhan Q 2009 *Adv. Opt. Photon.* **1** 1
[2] Halina R D, Andrew F, Berry M V, Dennis M R, David L A, Masud M, Cornelia D, Christina A, Peter B, Thomas B, Ebrahim K, Lorenzo M, Miles P, Monika R M, Natalia M L, Nicholas P B, Rosales-Guzmán C, Belmonte A, Torres J P, Tyler W N, Mark B, Reuven G, Alexander B S, Jacquiline R, Andrew G W, Robert F, Alan E W, Guodong X, Benjamin M and Andrew M W 2017 *J. Opt.* **19** 013001
[3] Quabis S, Dorn R, Eberler M, Glöckl O and Leuchs G 2000 *Opt. Commun.* **179** 1
[4] Youngworth K and Brown T 2000 *Opt. Express* **7** 77
[5] Zhan Q W and Leger J R 2002 *Opt. Express* **10** 324
[6] Dorn R, Quabis S and Leuchs G 2003 *Phys. Rev. Lett.* **91** 233901
[7] Wang H, Shi L, Lukyanchuk B, Sheppard C and Chong C T 2008 *Nat. Photon.* **2** 501
[8] Xie X, Chen Y, Yang K and Zhou J 2014 *Phys. Rev. Lett.* **113** 263901
[9] Wang X, Chen J, Li Y, Ding J, Guo C and Wang H 2010 *Phys. Rev. Lett.* **105** 253602
[10] Hnatovsky C, Shvedov V, Krolikowski W and Rode A 2011 *Phys. Rev. Lett.* **106** 123901
[11] Bautista G and Kauranen M 2016 *ACS Photon.* **3** 1351

[12] Nieminen T A, Heckenberg N R and Rubinsztein-Dunlop H 2008 *Opt. Lett.* **33** 122
[13] Cai M Q, Li P P, Feng D, Pan Y, Qian S X, Li Y, Tu C and Wang H T 2016 *Opt. Lett.* **41** 1474
[14] Li X, Cao Y and Gu M 2011 *Opt. Lett.* **36** 2510
[15] Wang S, Cao Y and Li X 2017 *Opt. Lett.* **42** 5050
[16] Gu B, Rui G, Xue Y, He J and Cui Y 2016 *J. Opt. Soc. Am. B* **33** 2512
[17] Xiao F, Ren Y, Shang W, Zhu W, Han L, Lu H, Mei T, Premaratne M and Zhao J 2018 *Opt. Lett.* **43** 3413
[18] Xiao F, Shang W, Zhu W, Han L, Premaratne M, Mei T and Zhao J 2018 *Photon. Res.* **6** 157
[19] Shang W, Xiao F, Han L, Premaratne M, Mei T and Zhao J 2018 *J. Phys.: Condens. Matter* **30** 064004
[20] Gong L, Gu B, Rui G, Cui Y, Zhu Z and Zhan Q 2018 *Photon. Res.* **6** 138
[21] Wang J 2016 *Photon. Res.* **4** B14
[22] Milione G, Nguyen T A, Leach J, Nolan D A and Alfano R R 2015 *Opt. Lett.* **40** 4887
[23] Janet C A P, Rajesh K B, Udhayakumar M, Jaroszewicz Z and Pillai T V S 2016 *Chin. Phys. Lett.* **33** 124206
[24] Prabakaran K, Rajesh K B, Sumathira S, Bharathi M D, Hemamalini R, Musthafa A M and Aroulmoji V 2016 *Chin. Phys. Lett.* **33** 094203
[25] Sundaram C M, Prabakaran K, Anbarasan P M, Rajesh K B and Musthafa A M 2016 *Chin. Phys. Lett.* **33** 064203
[26] Li P, Liu S, Zhang Y, Han L, Wu D, Cheng H, Qi S, Guo X and Zhao J 2017 *Front. Optoelectron.*
[27] Lin J, Yin K, Li Y and Tan J 2011 *Opt. Lett.* **36** 1185
[28] Chen Z and Zhao D 2012 *Opt. Lett.* **37** 1286
[29] Qin F, Huang K, Wu J, Jiao J, Luo X, Qiu C and Hong M 2015 *Sci. Rep.* **5** 9977
[30] Chen G Y, Song F and Wang H T 2013 *Opt. Lett.* **38** 3937
[31] Zhao Y, Edgar J S, Jeffries G D M, McGloin D and Chiu D T 2007 *Phys. Rev. Lett.* **99** 073901
[32] Bokor N and Davidson N 2004 *Opt. Lett.* **29** 1968
[33] Wang X L, Ding J, Ni W J, Guo C S and Wang H T 2007 *Opt. Lett.* **32** 3549
[34] Liu S, Qi S, Zhang Y, Li P, Wu D, Han L and Zhao J 2018 *Photon. Res.* **6** 228
[35] Zhang Y, Li P, Ma C, Liu S, Cheng H, Han L and Zhao J 2017 *Appl. Opt.* **56** 4956
[36] Zhang W, Huang L, Wei K, Li P, Jiang B, Mao D, Gao F, Mei T, Zhang G and Zhao J 2016 *Opt. Express* **24** 10376
[37] Machavariani G, Lumer Y, Moshe I, Meir A and Jackel S 2007 *Opt. Lett.* **32** 1468
[38] Naidoo D, Roux F S, Dudley A, Litvin I, Piccirillo B, Marrucci L and Forbes A 2016 *Nat. Photon.* **10** 327
[39] Li P, Zhang Y, Liu S, Ma C, Han L, Cheng H and Zhao J 2016 *Opt. Lett.* **41** 2205
[40] Qian S X, Kong L J, Li Y, Tu C and Wang H T 2014 *Opt. Lett.* **39** 1917
[41] Han L, Liu S, Li P, Zhang Y, Cheng H, Gan X and Zhao J 2016 *Appl. Opt.* **55** 9049
[42] Zhao C, Gan X, Li P, Fang L, Han L, Tu L and Zhao J 2016 *J. Lightwave Technol.* **34** 1206
[43] Gu B, Wen B, Rui G, Xue Y, Zhan Q and Cui Y 2016 *Opt. Lett.* **41** 1566
[44] Gu B, Wen B, Rui G, Xue Y, He J, Zhan Q and Cui Y 2016 *Opt. Express* **24** 25867
[45] Aiello A, Banzer P, Neugebauer M and Leuchs G 2015 *Nat. Photon.* **9** 789
[46] Antognozzi M, Bermingham C R, Harniman R L, Simpson S, Senior J, Hayward R, Hoerber H, Dennis M R, Bekshaev A Y, Bliokh K Y and Nori F 2016 *Nat. Phys.* **12** 731
[47] Aiello A, Marquardt C and Leuchs G 2010 *Phys. Rev. A* **81** 053838
[48] Neugebauer M, Banzer P, Bauer T, Orlov S, Lindlein N, Aiello A and Leuchs G 2014 *Phys. Rev. A* **89** 013840
[49] Aiello A, Lindlein N, Marquardt C and Leuchs G 2009 *Phys. Rev. Lett.* **103** 100401
[50] Liu Y, Ke Y, Luo H and Wen S 2016 *Nanophotonics* **6** 51
[51] Marrucci L, Manzo C and Paparo D 2006 *Phys. Rev. Lett.* **96** 163905
[52] Cardano F and Marrucci L 2015 *Nat. Photon.* **9** 776
[53] Lorenzo M, Ebrahim K, Sergei S, Bruno P, Enrico S, Eleonora N and Fabio S 2011 *J. Opt.* **13** 064001
[54] Yan L, Gregg P, Karimi E, Rubano A, Marrucci L, Boyd R and Ramachandran S 2015 *Optica* **2** 900
[55] Kim J, Li Y, Miskiewicz M N, Oh C, Kudenov M W and Escuti M J 2015 *Optica* **2** 958
[56] Bomzon Z e, Biener G, Kleiner V and Hasman E 2002 *Opt. Lett.* **27** 285
[57] Chen S, Zhou X, Liu Y, Ling X, Luo H and Wen S 2014 *Opt. Lett.* **39** 5274
[58] Glybovski S B, Tretyakov S A, Belov P A, Kivshar Y S and Simovski C R 2016 *Phys. Rep.* **634** 1
[59] Minovich A E, Miroshnichenko A E, Bykov A Y, Murzina T V, Neshev D N and Kivshar Y S 2015 *Laser Photon. Rev.* **9** 195
[60] Liu S, Li P, Zhang Y, Gan X, Wang M and Zhao J 2016 *Sci. Rep.* **6** 20774
[61] Gorodetski Y, Biener G, Niv A, Kleiner V and Hasman E 2005 *Opt. Lett.* **30** 2245
[62] Biener G, Gorodetski Y, Niv A, Kleiner V and Hasman E 2006 *Opt. Lett.* **31** 1594
[63] Chiao R Y and Wu Y S 1986 *Phys. Rev. Lett.* **57** 933
[64] Biener G, Niv A, Kleiner V and Hasman E 2002 *Opt. Lett.* **27** 1875
[65] Galvez E J, Crawford P R, Sztul H I, Pysher M J, Haglin P J and Williams R E 2003 *Phys. Rev. Lett.* **90** 203901
[66] Berry M V 1987 *J. Mod. Opt.* **34** 1401
[67] Chen H, Ling X H, Chen Z H, Li Q G, Lv H, Yu H Q and Yi X N 2016 *Chin. Phys. B* **25** 074201
[68] Liu S, Li P, Peng T and Zhao J 2012 *Opt. Express* **20** 21715
[69] Ke Y, Liu Y, Zhou J, Liu Y, Luo H and Wen S 2016 *Appl. Phys. Lett.* **108** 101102
[70] Karimi E, Slussarenko S, Piccirillo B, Marrucci L and Santamato E 2010 *Phys. Rev. A* **81** 053813
[71] Slussarenko S, Alberucci A, Jisha C P, Piccirillo B, Santamato E, Assanto G and Marrucci L 2016 *Nat. Photon.* **10** 571
[72] Alberucci A, Jisha C P, Marrucci L and Assanto G 2016 *ACS Photon.* **3** 2249
[73] Bomzon Z E, Biener G, Kleiner V and Hasman E 2002 *Opt. Lett.* **27** 1141
[74] Yin X, Ye Z, Rho J, Wang Y and Zhang X 2013 *Science* **339** 1405
[75] Ling X, Zhou X, Yi X, Shu W, Liu Y, Chen S, Luo H, Wen S and Fan D 2015 *Light Sci. Appl.* **4** e290
[76] Onoda M, Murakami S and Nagaosa N 2004 *Phys. Rev. Lett.* **93** 083901
[77] Hosten O and Kwiat P 2008 *Science* **319** 787
[78] Zhang Y, Li P, Liu S, Han L, Cheng H and Zhao J 2016 *Appl. Phys. B* **122** 1
[79] Gorodetski Y, Biener G, Niv A, Kleiner V and Hasman E 2006 *Opt. Commun.* **266** 365
[80] Hasman E, Kleiner V, Biener G and Niv A 2003 *Appl. Phys. Lett.* **82** 328
[81] Chen X, Chen M, Mehmood M Q, Wen D, Yue F, Qiu C W and Zhang S 2015 *Adv. Opt. Mater.* **3** 1201
[82] Zhang Y, Li P, Liu S and Zhao J 2015 *Opt. Lett.* **40** 4444
[83] Wang X L, Lou K, Chen J, Gu B, Li Y and Wang H T 2011 *Phys. Rev. A* **83** 063813
[84] Ling X, Yi X, Zhou X, Liu Y, Shu W, Luo H and Wen S 2014 *Appl. Phys. Lett.* **105** 151101
[85] Hamazaki J, Mineta Y, Oka K and Morita R 2006 *Opt. Express* **14** 8382
[86] Baumann S, Kalb D, MacMillan L and Galvez E 2009 *Opt. Express* **17** 9818
[87] Philip G M, Kumar V, Milione G and Viswanathan N K 2012 *Opt. Lett.* **37** 2667
[88] Zhang Y, Guo X, Han L, Li P, Liu S, Cheng H and Zhao J 2017 *Opt. Express* **25** 25725
[89] Chen H, Yu Z, Hao J, Chen Z, Xu J, Ding J and Wang H T 2014 *Appl. Phys. B* **114** 355
[90] Li X, Venugopalan P, Ren H, Hong M and Gu M 2014 *Opt. Lett.* **39** 5961
[91] Wang S, Li X, Zhou J and Gu M 2014 *Opt. Lett.* **39** 5022
[92] Nye J F 1999 *Natural Focusing and Fine Structure of Light: Caustics and Wave Dislocations* (Bristol: Institute of Physics Publishing)
[93] Aleahmad P, Miri M A, Mills M S, Kaminer I, Segev M and Christodoulides D N 2012 *Phys. Rev. Lett.* **109** 203902
[94] Chremmos I D, Chen Z, Christodoulides D N and Efremidis N K 2012 *Opt. Lett.* **37** 5003

[95] Vetter C, Eichelkraut T, Ornigotti M and Szameit A 2014 *Phys. Rev. Lett.* **113** 183901
[96] Zhang P, Hu Y, Li T, Cannan D, Yin X, Morandotti R, Chen Z and Zhang X 2012 *Phys. Rev. Lett.* **109** 193901
[97] Zhao J, Zhang P, Deng D, Liu J, Gao Y, Chremmos I D, Efremidis N K, Christodoulides D N and Chen Z 2013 *Opt. Lett.* **38** 498
[98] Wen Y, Chen Y, Zhang Y and Yu S 2017 *Chin. Opt. Lett.* **15** 030011
[99] Li P, Liu S, Peng T, Xie G, Gan X and Zhao J 2014 *Opt. Express* **22** 7598
[100] Siviloglou G A, Broky J, Dogariu A and Christodoulides D N 2007 *Phys. Rev. Lett.* **99** 213901
[101] Liu S, Wang M, Li P, Zhang P and Zhao J 2013 *Opt. Lett.* **38** 2416
[102] Zhang Y, Li P, Liu S, Han L, Cheng H and Zhao J 2016 *Opt. Express* **24** 28409
[103] Baumgartl J, Mazilu M and Dholakia K 2008 *Nat. Photon.* **2** 675
[104] Chen R P, Chen Z, Gao Y, Ding J and He S 2017 *Laser Photon. Rev.* **11** 1700165
[105] Li P, Liu S, Xie G, Peng T and Zhao J 2015 *Opt. Express* **23** 7131
[106] Li P, Liu S, Zhang Y, Xie G and Zhao J 2015 *J. Opt. Soc. Am. B* **32** 1867
[107] Liu Y, Ke Y, Zhou J, Luo H and Wen S 2015 *Opt. Express* **23** 16682
[108] Jiao X, Liu S, Wang Q, Gan X, Li P and Zhao J 2012 *Opt. Lett.* **37** 1041
[109] Zhang W, Liu S, Li P, Jiao X and Zhao J 2013 *Opt. Express* **21** 974
[110] Li P, Guo X, Qi S, Han L, Zhang Y, Liu S, Li Y and Zhao J 2018 *Sci. Rep.* **8** 9831
[111] Gao X Z, Pan Y, Li S M, Wang D, Li Y, Tu C and Wang H T 2016 *Phys. Rev. A* **93** 033834
[112] Li P, Zhang Y, Liu S, Han L, Cheng H, Yu F and Zhao J 2016 *Opt. Lett.* **41** 4811
[113] Moreno I, Davis J A, SánchezL ópez M M, Badham K and Cottrell D M 2015 *Opt. Lett.* **40** 5451
[114] Davis J A, Moreno I, Badham K, SánchezL ópez M M and Cottrell D M 2016 *Opt. Lett.* **41** 2270
[115] Li P, Zhang Y, Liu S, Cheng H, Han L, Wu D and Zhao J 2017 *Opt. Express* **25** 5821
[116] Fu S, Zhang S and Gao C 2016 *Sci. Rep.* **6** 30765
[117] Li P, Wu D, Zhang Y, Liu S, Li Y, Qi S and Zhao J 2018 *Photon. Res.* **6** 756
[118] Corato-Zanarella M, Dorrah A H, Zamboni-Rached M and Mojahedi M 2018 *Phys. Rev. Appl.* **9** 024013
[119] Bickel W S and Bailey W M 1985 *Am. J. Phys.* **53** 468
[120] McMaster W H 1954 *Am. J. Phys.* **22** 351
[121] Durnin J 1987 *J. Opt. Soc. Am. A* **4** 651
[122] Chávez-Cerda S, Tepichin E, Meneses-Nava M A, Ramirez G and Hickmann J M 1998 *Opt. Express* **3** 524
[123] Čižmár T, Kollárová V, Bouchal Z and Zemánek P 2006 *New J. Phys.* **8** 43
[124] Mazilu M, Stevenson D J, Gunn-Moore F and Dholakia K 2009 *Laser Photon. Rev.* **4** 529
[125] Orlov S, Regelskis K, Smilgevičius V and Stabinis A 2002 *Opt. Commun.* **209** 155
[126] Niv A, Biener G, Kleiner V and Hasman E 2004 *Opt. Lett.* **29** 238
[127] Ruffner D B and Grier D G 2012 *Phys. Rev. Lett.* **109** 163903
[128] Wu G, Wang F and Cai Y 2014 *Phys. Rev. A* **89** 043807
[129] Čižmár T and Dholakia K 2009 *Opt. Express* **17** 15558
[130] Zamboni-Rached M 2004 *Opt. Express* **12** 4001
[131] Vieira T A, Gesualdi M R R and Zamboni-Rached M 2012 *Opt. Lett.* **37** 2034
[132] Dorrah A H, Zamboni-Rached M and Mojahedi M 2017 *Appl. Phys. Lett.* **110** 051104
[133] Wang X L, Li Y N, Chen J, Guo C S, Ding J P and Wang H T 2010 *Opt. Express* **18** 10786
[134] Milione G, Sztul H I, Nolan D A and Alfano R R 2011 *Phys. Rev. Lett.* **107** 053601
[135] Ling X, Yi X, Dai Z, Wang Y and Chen L 2016 *J. Opt. Soc. Am. B* **33** 2172
[136] Fang X, MacDonald K F, Plum E and Zheludev N I 2016 *Sci. Rep.* **6** 31141
[137] Tang Y and Cohen A E 2011 *Science* **332** 333
[138] Vyas S, Kozawa Y and Miyamoto Y 2015 *Opt. Express* **23** 33970
[139] Adams C S and Riis E 1997 *Prog. Quant. Electron.* **21** 1
[140] Hopkins S A and Durrant A V 1997 *Phys. Rev. A* **56** 4012
[141] Anderson W R, Bradley C C, McClell, J J and Celotta R J 1999 *Phys. Rev. A* **59** 2476
[142] Brzobohatý O, Arzola A V, Šiler M, Chvátal L, Jákl P, Simpson S and Zemánek P 2015 *Opt. Express* **23** 7273
[143] Ramanathan A, Wright K C, Muniz S R, Zelan M, Hill W T, Lobb C J, Helmerson K, Phillips W D and Campbell G K 2011 *Phys. Rev. Lett.* **106** 130401
[144] Otte E, Rosales-Guzmán C, Ndagano B, Denz C and Forbes A 2018 *Light Sci. Appl.* **7** 18009
[145] Fickler R, Lapkiewicz R, Ramelow S and Zeilinger A 2014 *Phys. Rev. A* **89** 060301
[146] Galvez E J, Khadka S, Schubert W H and Nomoto S 2012 *Appl. Opt.* **51** 2925
[147] Feng S and Winful H G 2001 *Opt. Lett.* **26** 485
[148] Wang J, Wang L, Xin Y and Song M 2017 *J. Opt. Soc. Am. A* **34** 1924
[149] Cardano F, Karimi E, Marrucci L, de Lisio C and Santamato E 2013 *Opt. Express* **21** 8815
[150] Vyas S, Kozawa Y and Sato S 2013 *Opt. Express* **21** 8972
[151] Baumann S M, Kalb D M, MacMillan L H and Galvez E J 2009 *Opt. Express* **17** 9818
[152] Zhu W, Shvedov V, She W and Krolikowski W 2015 *Opt. Express* **23** 34029
[153] Han L, Liu S, Li P, Zhang Y, Cheng H and Zhao J 2018 *Phys. Rev. A* **97** 053802
[154] Bliokh K Y and Nori F 2015 *Phys. Rep.* **592** 1
[155] Bauer T, Banzer P, Karimi E, Orlov S, Rubano A, Marrucci L, Santamato E, Boyd R W and Leuchs G 2015 *Science* **347** 964
[156] Jo J S, Milster T D and Erwin J K 2002 *Opt. Eng.* **41** 1866
[157] Kozawa Y and Sato S 2006 *Opt. Lett.* **31** 820
[158] Lerman G M, Stern L and Levy U 2010 *Opt. Express* **18** 27650
[159] Cheng H, Li P, Liu S, Chen P, Han L, Zhang Y, Hu W and Zhao J 2017 *Appl. Phys. Lett.* **111** 141901
[160] Friese M E J, Nieminen T A, Heckenberg N R and Rubinsztein-Dunlop H 1998 *Nature* **394** 348
[161] Sick B, Hecht B and Novotny L 2000 *Phys. Rev. Lett.* **85** 4482
[162] Li X, Lan T H, Tien C H and Gu M 2012 *Nat. Commun.* **3** 998
[163] Abouraddy A F and Toussaint K C 2006 *Phys. Rev. Lett.* **96** 153901
[164] Chen W and Zhan Q 2010 *J. Opt.* **12** 045707
[165] Zhu W and She W 2013 *Opt. Express* **21** 17265
[166] Rodrigo J A, Alieva T, Abramochkin E and Castro I 2013 *Opt. Express* **21** 20544
[167] Zhang G L, Gao X Z, Pan Y, Zhao M D, Wang D, Zhang H H, Li Y, Tu C and Wang H T 2018 *Opt. Express* **26** 16782
[168] Chen Z, Zeng T and Ding J 2016 *Opt. Lett.* **41** 1929
[169] Chang C, Gao Y, Xia J, Nie S and Ding J 2017 *Opt. Lett.* **42** 3884
[170] Mushiake Y, Matsumura K and Nakajima N 1972 *Proc. IEEE* **60** 1107
[171] Mao D, Feng T, Zhang W, Lu H, Jiang Y, Li P, Jiang B, Sun Z and Zhao J 2017 *Appl. Phys. Lett.* **110** 021107